Separation of scales in fracture mechanics. From molecular to continuum theory *via* Γ-convergence.

M. S. GELLI
Scuola Normale Superiore
Piazza dei Cavalieri 7, 56126 Pisa, Italy

G. F. ROYER-CARFAGNI
Dipartimento di Ingegneria Civile, Università di Parma
Parco Area della Scienze 181/A, 43100 Parma, Italy

November 22, 2001

Abstract

We propose a procedure to obtain a consistent mesh-objective continuous model, starting from discrete chains of elements allowing for strain softening. Observing the size-dependent response of tensile chains, and extrapolating the scaling law as the number of constituents goes to infinity, we use recent results of variational convergence of discrete functionals (Γ-convergence) to pass from a molecular to a continuum theory. The limit model, where softening and fracture are interpreted by the dichotomy of bulk and surface energies, reproduces the same overall properties of discrete systems.

1 Introduction

Description of fracture process by means of continuum models has gained wide popularity in recent years. Their main advantage is that they can be easily implemented in a FEM code, a characteristic particularly helpful in the design practice of structures made of brittle or quasi-brittle materials.

For, it is supposed that many small cracks are distributed (*smeared*) over a representative volume element, so that the effect of cracking can be modelled through a simple constitutive relationship between strain and stress. Since the wider the crack opening, the lower are the cohesive forces bridging the crack surfaces, the material stiffness gradually decays after a peak load has been reached. Consequently, the constitutive relation usually presents a strain-softening branch, which approaches the zero value when a passing-through crack has fully developed.

However, consideration of continua with softening leads to some theoretical difficulties which, yet, appear to be still partially unappreciated. The simplest way to illustrate may be to refer to a one-dimensional example. Consider a bar of length L extended in a hard device. Introduced the x-axis such that $\Omega \equiv (0, L) \subset \mathbb{R}$ denotes the bar undistorted natural reference configuration, let $u(x) : \Omega \to \mathbb{R}$ represent the displacement of a particle initially at x. Suppose that the material is *non linear elastic*, obeying to a strain-softening constitutive relationship, between the axial load $\sigma(x)$ and the axial strain $\varepsilon(x) \equiv u'(x)$, of the type represented in Figure 1a. When the bar extremities are displaced apart of $\beta L > 0$, the variational form of the problem is

$$\min_u \int_0^L U(u'(x))\, dx\,, \quad u(L) - u(0) = \beta L\ , \tag{1}$$

where the strain energy U has the shape represented in Figure 1(b). It is clear that strain softening corresponds to concavity for U so that, in general, problem (1) is one of non-convex minimization.

Traditionally, constitutive relationship with softening branches (or their integral representation through non-convex energies) have been employed to model material phase transitions, such as the vapor-liquid transition in water predicted by van der Waals equation [18]. In the late '70s, fundamental papers by Ericksen [15] and Dunn & Fosdick [14] showed that the response of some solid materials exhibiting strain softening, could similarly be interpreted as equilibrium-state sequences of heterogenous configurations, composed of two (or more) material phases. Each phase corresponds to an underlying rearrangement at the microscopic level, and phase-equilibrium is amenable to description through non-convex minimization. An example of this is the approach proposed by Müller and Villaggio in [20], where the elastic-plastic transition in a solid body is explained through snap-through spring devices, governed by non-convex strain energies.

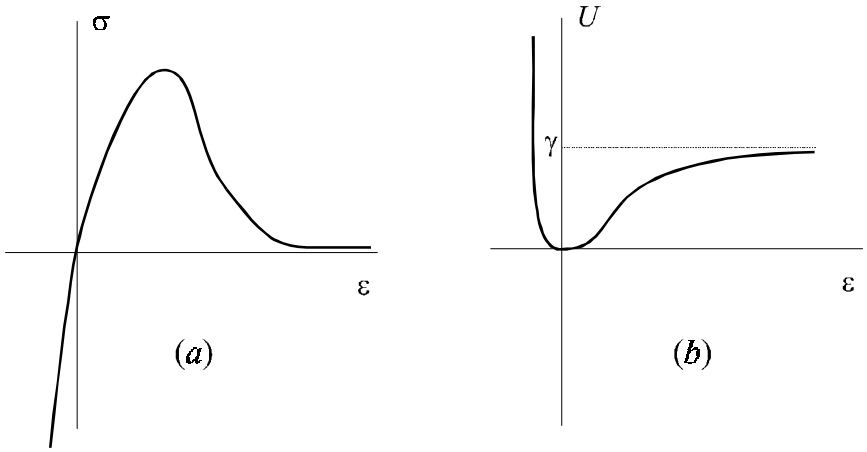

Figure 1: Softening constitutive relationship (a) and the corresponding strain energy function (b).

Recently, starting from an important paper by Truskinovsky [23], the phase-transition framework has been addressed to fracture mechanics. In particular, as shown in [23], whenever the strain energy presents a horizontal asymptote (as in Figure 1b), equilibrium may be characterized by *localization* of exceptionally large strains in layers of evanescent thickness, equivalent to surfaces of discontinuity (fractures) for the deformation field. But there is a troublesome consequence: the energy necessary to produce a fracture in a continuous bar with strain-softening results to be zero, whatever the level of the horizontal asymptote in the strain potential. Indeed, the problem[1] in the minimization of (1) is due to a congenital mathematical difficulty, already realized in the early work by Bolza and Young [24]. In fact, using direct methods in the calculus of variations, it could be verified that, for any $\beta > 0$, we can find sequences u_n of continuous functions, such that $u_n(L) - u_n(0) = \beta L$ and

$$\lim_{n\to\infty} \int_0^L U(u_n') = 0\,.$$

The study of strain localization and the consequent disappearance of fracture energy is nowadays a topical subject, especially because of the fatal con-

[1] As discussed [22], a similar problem occurs when trying to describe flexure of softening beams through a moment-curvature relationship.

sequences in FEM numerical approximations [19]. To illustrate the problem in engineering terms, it is convenient to follow the same approach reported by Bažant and Planas ([5], Sections 8.1-8.2), by considering an approximate formulation of (1). Suppose that the bar is covered by N elements of length L/N. Evaluating the strain in the i-th element as the ratio between the displacements u_{i+1} and u_i at its extremities and the element length L/N, the total strain energy in the bar may be tentatively approximated by

$$\mathcal{E}^N = \sum_{i=0}^{N} \frac{L}{N} U\left((u_{i+1} - u_i)/(L/N)\right) \ , \ \ u_N - u_0 = \beta L \ , \tag{2}$$

with $u_0 \equiv u(0)$ and $u_N \equiv u(L)$.

Minimization of $\mathcal{E}^N$ subjected to condition $u_N - u_0 = \beta L$ leads to the aforementioned striking conclusion. Referring to ([5], Section 8.1.4) for more details, just observe that breaking of one element corresponds to an energy consumption equal to $\gamma L/N$, where γ is the level of the horizontal asymptote in Figure 1*b* (equal to the area under the positive branch of the graph in Figure 1*a*). Since rupture of one element implies rupture of the whole bar, we observe that the resulting fracture energy $\gamma L/N$ decreases with increasing N, approaching zero as $N \to \infty$. Consequently, the bar response depends upon the size of the employed mesh or, in other words, is *mesh-unobjective*. Verbatim from [5], the foregoing example *"shows that the simple stress-strain model with strain softening leads to unacceptable behavior both physically and computationally: (1) the softening zone has a zero width and volume; (2) the inelastic strain and fracture work are zero; and (3) the computational results are mesh objective. [...] The conclusion is that these models*[2] *are not suitable at all because they allow localization in a region of zero volume"*

In order to overcome this difficulty, a commonly accepted procedure, at least at the numerical level, consists in complementing the continuum problem with particular conditions, which prevent the strain from localizing into vanishing regions. Such conditions are generically referred to as *localization limiters* [2], among which Bažant's crack band model [5] represents a well-known example in engineering applications. In a variational approach, localization limiters can be set by complementing the bulk energy F, function of the strain $\varepsilon(x) \equiv u'(x)$, with a cohesive fracture energy G, function of the

[2] The discrepancies between discrete and continuum models with non-convex energies, already noted by Bažant in [1], has been more recently discussed by Rogers and Truskinovsky [21].

displacement discontinuity (fracture opening). The problem may be stated in the form

$$\min_u \int_0^L F(u'(x))\,dx + \sum_{x_j \in J_u} G([u](x_j))\,, \quad u(L) - u(0) = \beta L\,, \tag{3}$$

where J_u denotes the set of discontinuity points of u and $[u](x_j)$ represents the jump of u at x_j.

In general, one should be able to define F and, what is more, G starting from chains of discrete elements, obeying to strain-softening constitutive relationships similar to that of Figure 1*a*. To this aim, many different approaches have been proposed, but they usually come up against the main difficulty evidenced in the foregoing example: passing to the limit as the length of the constituent elements goes to zero, it is trivially found that $G \equiv 0$. A successful strategy has been recently proposed by Braides *et. al.* [9], who mathematically demonstrated that, in order to avoid in the limit the trivial case $G \equiv 0$, it is sufficient to assume that the elementary response depends upon the size of the elementary constituents. In other words, the constitutive relationship should depend upon the size of the segments forming the chain. However, despite the mathematical soundness of the procedure, to our knowledge the physical justification of such a scaling, indeed the crucial point, has yet to be justified.

The aim of this paper is to contribute to clarify the scaling laws by proposing a mechanically-motivated procedure where, starting from discrete ensembles of elements, we attain the behavior of a continuous softening bar by letting the length of each element tend to zero and the number of elements to infinity. The key point is to observe that the limit process cannot avoid to consider the size effect in the material behavior [4], i.e. the dependence of the structural response upon the size of the body. For, developing early ideas by Truskinovsky [23], we start by studying the behavior of bars made up of chains of interacting atoms, observing in particular the size-dependence of their response as the atom number is varied. From the proper definition of a discretization-size-dependent constituent-law, we will use recent results in the calculus of variations (Γ-convergence of discrete schemes [7]) to get rid of this dependence by performing an asymptotic limit (Γ-limit). This operation will let us pass to a continuum model preserving most of the characteristic properties of the discrete ensemble, in particular presenting finite fracture energy. The technique of introducing localization limiters thus acquires a consistent interpretation from this more general point of view.

2 Scaling laws in bars

To illustrate our method, we start from the simple example of a string of atoms, represented by material points having one degree of freedom as if they were aligned on a frictionless rod. We may assume, at least as a first-order approximation, that the forces between any two atoms depend upon their relative distance only, and that the radius of the sphere of atomic activity is of the order of atomic spacing (nearest-neighbor interaction). Thus, the interaction is equivalent to the effect of (non-linear) elastic springs, connecting in pairs any two contiguous atoms.

Introduced a reference axis x, let u_i denote the displacement in the positive direction of the i-th atom at $x = x_i$. In the simplest case, suppose that the force between two neighboring atoms i and $i+1$ can be represented by a Griffith-type interaction potential

$$\lambda\Psi_1\left(\frac{u_{i+1}-u_i}{\lambda}\right) = \begin{cases} \lambda\, a\,[(u_{i+1}-u_i)/\lambda]^2 & \text{for } (u_{i+1}-u_i)/\lambda < \varepsilon_1\,, \\ \lambda\,\gamma_1 & \text{for } (u_{i+1}-u_i)/\lambda \geq \varepsilon_1\,, \end{cases} \tag{4}$$

where λ represents the natural undistorted interatomic distance and $\varepsilon_1 \equiv \sqrt{\gamma_1/a}$. The graph of $\Psi_1(\cdot)$, representing the potential per unit length, is drawn in Figure 2b, whereas Figure 2a shows the corresponding interatomic force $\sigma \equiv \Psi_1'$.

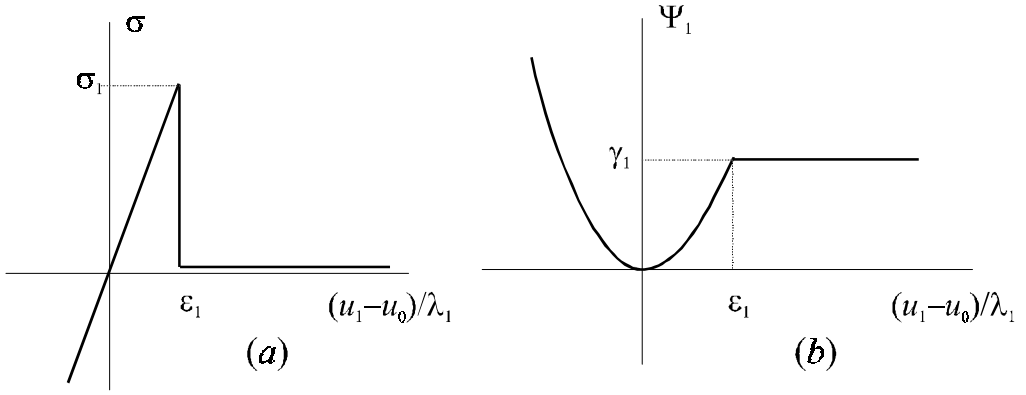

Figure 2: Next-neighbor-interaction atomic force (a) and corresponding atomic potential (b).

Consider first a chain composed of only three atoms. Supposing we give to its extremities the relative displacement $u_2 - u_0 = \beta(2\lambda)$, while the atom in the middle remains free to move, the ensemble energy is given by $(2\lambda)\Psi_2(\beta)$, where $\Psi_2(\beta)$ (the energy per-unit-length) reads

$$\Psi_2(\beta) = \min_{\frac{u_2-u_0}{2\lambda}=\beta} \frac{1}{2\lambda}\left[\lambda\Psi_1\left(\frac{u_2-u_1}{\lambda}\right) + \lambda\Psi_1\left(\frac{u_1-u_0}{\lambda}\right)\right] . \tag{5}$$

A simple calculation shows that the graph of $\Psi_2(\cdot)$ coincides with that of $\Psi_1(\cdot)$, except that it is truncated at $\gamma_2 \equiv \gamma_1/2$. In general, to a system of $k+1$ atoms constrained by $(u_k - u_0)/(k\lambda) = \beta$, we associate the energy $(k\lambda)\Psi_k(\beta)$, with

$$\Psi_k(\beta) = \min_{\frac{u_k-u_0}{k\,\lambda}=\beta} \frac{1}{k\,\lambda}\left[\sum_{i=1}^{k} \lambda\Psi_1\left(\frac{u_i-u_{i-1}}{\lambda}\right)\right] . \tag{6}$$

It is simple to calculate that (see for example [23], Section 3)

$$\Psi_k(\beta) = \begin{cases} \Psi_1(\beta) & \text{for } \beta < \varepsilon_k\,, \\ \\ \gamma_k & \text{for } \beta \geq \varepsilon_k\,, \end{cases} \qquad \text{with } \gamma_k \equiv \gamma_1/k\,,\ \varepsilon_k \equiv \sqrt{\gamma_k/a} = \varepsilon_1/\sqrt{k}\,. \tag{7}$$

The scaling of the graphs for varying k, reported in Figure 3, indicates the *size effect* in the chain response.

So far, we have considered the passage from a microscopic constituent to a mesoscopic ensemble. We now consider the inverse process, from "meso" to "micro". Let a chain of length L be composed of a great number of atoms spaced of λ, $L/\lambda \gg 1$, obeying to the same constitutive law described by Figure 2. From the aforementioned analysis, its tensile response is governed by the potential $(k\lambda)\Psi_k$, defined as in (7), with $k = L/\lambda$. Suppose that now we consider one half of the aforementioned chain, constituted by $k+1$ atoms where now $k = (L/2)/\lambda$. Its potential, because of the previous considerations, is again given by (7). As the length of the chain is decreased, the number of atoms it contains becomes smaller and smaller. The graph of the corresponding Ψ_k is represented in Figure 4 for $k = (L/n)/\lambda$, $n = 1, ..., 4$. What should be noticed is that the horizontal *plateau* reaches the level $\gamma_{L/n\lambda}$ and intersects the parabola at $\varepsilon_{L/n\lambda}$, where

$$\gamma_{L/n\lambda} = n\,\gamma_{L/\lambda} = n\frac{\lambda}{L}\gamma_1\ ,\ \ \varepsilon_{L/n\lambda} = \left(\frac{\gamma_{L/n\lambda}}{a}\right)^{1/2} = \left(n\frac{\gamma_{L/\lambda}}{a}\right)^{1/2} = (n)^{1/2}\varepsilon_{L/\lambda}\ . \tag{8}$$

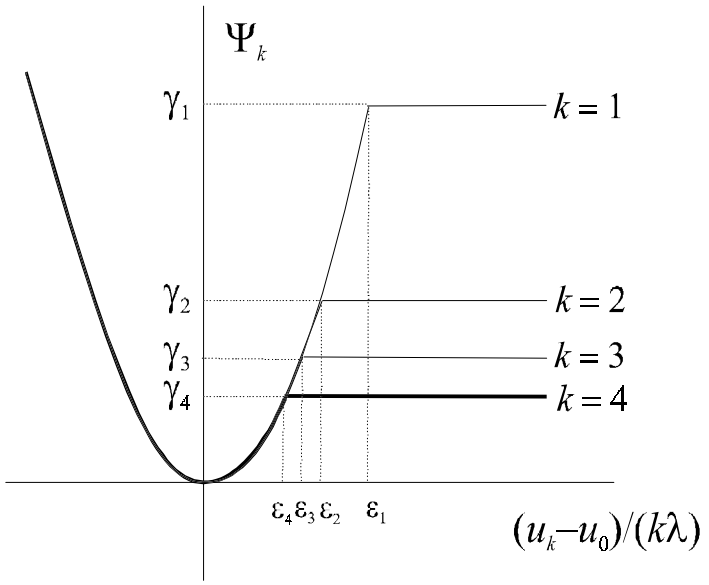

Figure 3: Energy per unit length of chains composed of $k+1$ atoms. Cases $k = 1 - 4$.

Thus, diminishing the length of the chain, the *plateau* becomes higher and higher and its intersection point with the convex basin moves rightward. The proper scaling, i.e. the rate of change of the representative parameters with specimen size, are given by formulas (8). Of course the *plateau* level cannot approach infinity since, at most, $n = L/\lambda$. Such value corresponds to the case in which the chain is composed of only two atoms. Increasing n beyond this value has no meaning, at least from a physical point of view.

The foregoing analysis has revealed important aspects that must be considered when passing from a molecular to a continuum theory:

1. Suppose that a body, conceived of as formed by a discrete number of elementary constituents, is divided into a certain number of portions (here, we have supposed to divide a long chain of atoms in a certain number of sub-chains). In order to obtain the same overall response for the whole body after assemblage, the potential per unit volume that must be considered for each portion is not fixed, but depends upon the size of the ideal subdivision or, in other words, is mesh-dependent. The scaling law, due to the structural size effect [5], for the case at hand, is

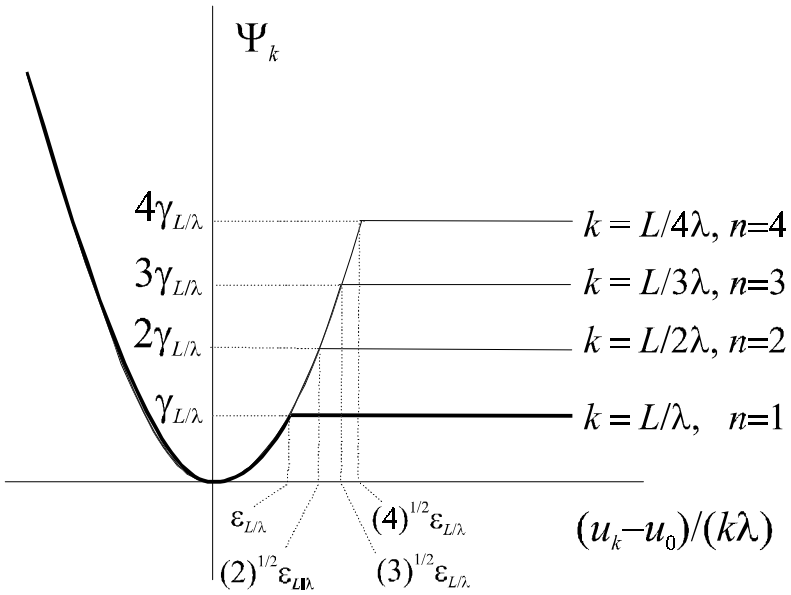

Figure 4: Scaling law for a long atom chain divided in n parts.

given by (8) and represented in Figure 4.

2. The basin of stability for the interaction energy density, as well as the minimum value characterizing the unstable region, must grow at a suitable rate as the size of the ideal subdivision is reduced. For the atom chain here considered, the scaling rate is indicated by the parameters $\gamma_{L/n\lambda}$ and $\varepsilon_{L/n\lambda}$ referred to in (8).

3. In general, the energy does not grow unboundedly since the ideal subdivision cannot be finer than the characteristic size of the smaller representative volume element. In our example, the element subdivision could not be smaller than the interatomic spacing λ, that is $n \leq L/\lambda$.

All these steps have to be considered when passing from a discrete to a continuum model. In particular, (1) (2) and (3) will provide a motivation for conceiving a particular scaling of the potential, a key-hypothesis to obtain a finite surface energy in the limit, even though the volume fraction of surface atoms goes to zero. The idea of re-scaling the potential in order to ovoid disappearance of the fracture energy in the continuum limit was first advanced,

to our knowledge, by Truskinovsky in [23]. Here, Truskinovsky's original idea is re-interpreted and attributed to the size-effect of atomic chains, adapting to our particular case concepts and methods traditionally employed by design engineers for concrete and other quasi-brittle materials ([3] and [5] contain excellent state-of-the-art reviews).

3 From discrete to continuum

The foregoing analysis has allowed us to infer that the response of an atomic chain is governed by a discretization-size dependent (mesh dependent) constitutive law. For the representative example of Section 2, the scaling is indicated by the potential $\Psi_k(\cdot)$ defined in (7), with $k = \frac{1}{n}L/\lambda$, being L the total length of the chain and $\frac{1}{n}L$ the length of the sub-chain we are considering. Obviously, the subdivision cannot go beyond the interatomic distance, so that $n \leq L/\lambda$. Considering values for n beyond this bound is meaningless from a physical point of view; however, passing to the limit for $n \to \infty$ may have a mathematical significance.

In rough terms, extrapolating the scaling law beyond the threshold of physical acceptability ($n > L/\lambda$) follows the same strategy of a mathematical limit: we keep track of the trend *in a neighborhood* of the limit point, rather than the of the value *at* the limit point. This procedure may appear not completely rigorous, but the passage from molecular to continuum theory surely requires some hypotheses. In particular, in molecular theory the only significant parameters are the atom displacements, whose spacing is fixed and, consequently, it is difficult to define the displacement gradient as the limit of the corresponding difference quotients. In order to overcome these problems, we attempt the following strategy. We suppose to extend the scaling law, given by (7) for the case at hand, for $n \to \infty$ i.e. beyond the limit L/λ. The proper scaling law is the natural extension, for $n \to \infty$, of that obtained for the physically-meaningful cases. For example, we may consider formulas (7) with $k = \frac{1}{n}L/\lambda$ for any n, that is even for $k < 1$. We then define, through a suitable limiting process (Γ-limit) for $n \to \infty$ (recovering the convergence results of [7]) a limit energy functional which, remarkably, presents the following noteworthy features.

- The inelastic strain and fracture work of bars characterized by this energy do not disappear in the limit, but are equal to those corresponding to the borderline case of two interacting atoms.

- Track of possible softening branches in the interatomic force-displacement diagram is kept in the limit.
- The resulting model is set for displacement fields $u(x) : (0, L) \to \mathbb{R}$, i.e. for functions defined in a whole interval, rather than on a discrete set of points. In such a way, derivatives can replace the difference quotient.
- Possible fractures are modelled by discontinuities of $u(x)$.

Moreover, despite the numerical aspects are not discussed in this paper, we believe that, if properly implemented in a FEM framework, the model can provide mesh-objective results.

3.1 A Γ-convergence result and its mechanical interpretation

The general mathematical setting of the problem is the following. For a bar of length L, let $u(x)$ and $f(x)$ represent the displacement and the load per unit length at x. Considering an ideal subdivision of the bar in n parts of length L/n, delimited by the nodes $x_i = iL/n$, define

$$u_i \equiv u(x_i) \ , \quad x_i = i\, L/n \, , \ i = 0, ..., n \, , \tag{9}$$

and

$$f_i \equiv \int_{x_i - L/(2n)}^{x_i + L/(2n)} f(x)\, dx \ . \tag{10}$$

Following Section 2, let us suppose that the response of each constituent part of length L/n is characterized by an energy per unit length of the type

$$\Phi_n \left(\frac{u_i - u_{i-1}}{L/n} \right) \ , \tag{11}$$

where the pedex n evidences that such quantity depends upon n. Then, consider for the bar the sequence of energies

$$\mathcal{E}^n \left[\{u_i\}_{i=0}^n \right] \equiv \sum_{i=1}^{n} \frac{L}{n}\, \Phi_n \left(\frac{u_i - u_{i-1}}{L/n} \right) - \sum_{i=1}^{n-1} f_i\, u_i \, . \tag{12}$$

The functional (12) has a precise physical interpretation, i.e. $\mathcal{E}^n$ can be directly measured from a simple experiment. A testing device of the type schematically represented in Figure 5 could be used. In this apparatus, the bar AB is clamped at points $0, ..., i, .., n$ by special jaws, which have been firmly tightened to the specimen by fastening the apposite screws. The jaws are connected to the fixed support CD and when the bar is in its undistorted state, they are equidistant. Suppose that now the generic point i is displaced of the quantity u_i. Provided each jaw is equipped with a load cell, we can measure the work that is expended to give to points $0, .., i, .., n$ the displacements $u_0, .., u_i, ..., u_n$. Such value coincides with the first term on the right hand side of (12). Increasing the number of jaws, we can impose to the bar the displacement u_i at $x_i = iL/n$ for any n and measure the quantity $\Phi_n((u_i - u_{i-1})/(L/n))$. It should be remarked that no real experiment could ever be conceived to directly measure the stored energy $\mathcal{E}[u]$, corresponding to a continuous displacement field u. What instead is possible is to assign the displacements u_i to a *discrete* set of points and directly measure $\Phi_n((u_i - u_{i-1})/(L/n))$. By letting $n \to \infty$ we can approximate the stored energy function of a continuous bar.

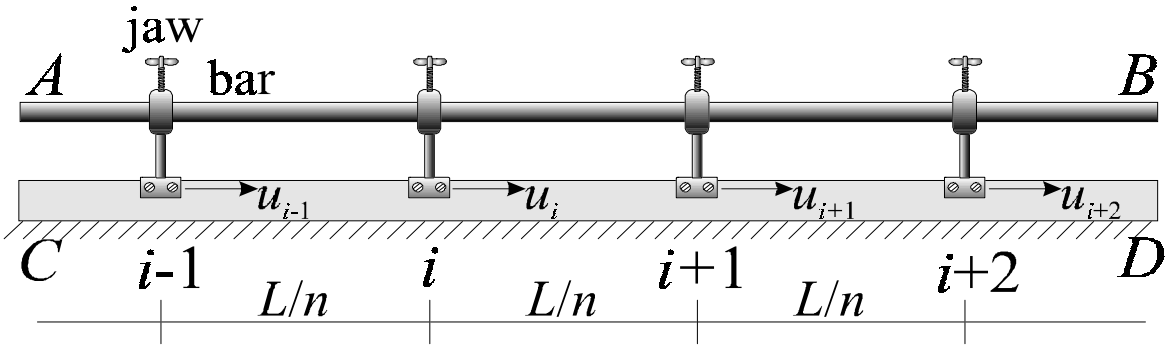

Figure 5: Clamping device to measure $\mathcal{E}^n$.

Let now $u(x) : (0, L) \to \mathbb{R}$ be a fixed function, possible candidate to represent the displacement field for a continuous bar. If $u(x)$ was continuous, using the device of Figure 5, we might think of increasing the number n of jaws and assign the displacements $u_i = u(iL/n)$, $i = 0, .., n$, while measuring the work expended in the process. However, if we allow for fractures, $u(x)$ may be discontinuous at some points, so that we must define a more general

and mathematically rigorous procedure. In the most general case, we suppose that $u \in SBV(0,L)$, i.e., $u(x)$ admits at most a countable set of discontinuity points, in the following referred to as J_u, and is differentiable a.e.[3] outside J_u. Moreover, denoting with $[u](x_j)$ the jump of u at x_j, and with $u'(x)$ the derivative of u at x (where defined), we must have

$$\int_0^L |u|\,dx < \infty \quad , \quad \int_0^L |u'|\,dx + \sum_{x_j \in J_u} |[u](x_j)| < \infty \,. \tag{13}$$

As a second step, despite the functional (12) depends only upon the nodal displacements $\{u_i\}$, it is useful to think of it as defined on the set of piecewise affine (continuous) functions $u_n : (0,L) \to \mathbb{R}$, obtained by linearly interpolating the nodal values $\{u_i\}_{i=0}^n$, i.e.

$$u_n(x) = u_{i-1}(x) + \frac{u_i - u_{i-1}}{L/n}(x - x_i) \;\text{ for }\; x \in (x_{i-1}, x_i)\,,\; i = 1,..,n\,. \tag{14}$$

Then we set, without ambiguity

$$\mathcal{E}^n[\{u_i\}_{i=0}^n] \equiv \mathcal{E}^n[u_n]\,. \tag{15}$$

For any $u \in SBV(0,L)$, we then consider sequences $u_n(x)$ approaching $u(x)$ "*in measure*", i.e.,

$$u_n \overset{meas}{\to} u \iff \forall \varepsilon > 0\,,\; \lim_{n\to\infty} meas\left(\{x \in (0,L) : |u_n(x) - u(x)| > \varepsilon\}\right) = 0\;, \tag{16}$$

where $meas(\Omega)$ denotes the (Lebesgue) measure of Ω. From a physical point of view, we allow that there might be even a great difference between $u_n(x)$ and $u(x)$, but the region where this happen must be confined in a vanishing set as $n \to \infty$. We define the energy $\mathcal{E}[u]$ as

$$\mathcal{E}[u] = \inf\left\{ \lim_{j\to+\infty} \inf_{n\geq j} \mathcal{E}^n[u_n] : \forall\; u_n \overset{meas}{\to} u \right\}\,, \tag{17}$$

usually referred to as the Γ-limit of $\mathcal{E}^n$ and denoted with $\mathcal{E}[u] = \Gamma\text{-}\lim_{n\to\infty} \mathcal{E}^n[u]$ (an elementary but exhaustive introduction to Γ-convergence can be found in [6]).

[3] With *a.e.* we mean *almost everywhere*, that is, everywhere except at most a set of zero Lebesgue measure.

The definition (17) is natural from a physical point of view. It is a consequence of assuming that the bar would naturally tend towards the minimum-energy configuration though any possible approximation[4] of u, obtained through assigning discrete nodal displacements in the sense of (16). Moreover, in the cases we treat, it can be proved that for any boundary value we have *convergence of minima*, that is

$$\min\left\{\mathcal{E}^n[v_n] : v_n(L) - v_n(0) = \beta L\right\} \underset{n\to\infty}{\to} \min\left\{\mathcal{E}[v] : v(L) - v(0) = \beta L\right\} . \tag{18}$$

Moreover, if v_n^* is a minimizer $\mathcal{E}^n$ in the admissible class, then for $n \to \infty$ we have, up to a subsequence,

$$v_n^* \overset{meas}{\to} v^* , \tag{19}$$

where v^* is a minimum point for $\mathcal{E}[v]$ in the admissible class, i.e. we have *convergence of minimizers.*

To state the main mathematical result, we suppose that $\Phi_n : \mathbb{R} \to \mathbb{R} \cup \{+\infty\}$ of (12), satisfies the following properties.

a) There exist upper and lower thresholds ε_n^+ and ε_n^-, with

$$\lim_{n\to\infty} \varepsilon_n^{\pm} = \pm\infty , \ \lim_{n\to\infty} \frac{\varepsilon_n^{\pm}}{n} = 0 , \tag{20}$$

such that $\Phi_n(z)$ is concave when restricted to either $(-\infty, \varepsilon_n^-)$ or $(\varepsilon_n^+, +\infty)$.

b) There exist constants $a > 0$, $p > 1$ and $C > 0$ such that

$$\Phi_n(z) \geq a(|z|^p - 1) , \ \forall z \in (\varepsilon_n^-, \varepsilon_n^+) , . \tag{21}$$

$$\frac{1}{n}\Phi_n(z) \geq C > 0 , \ \forall z \notin (\varepsilon_n^-, \varepsilon_n^+) . \tag{22}$$

c) Defined

$$F_n(z) \equiv \begin{cases} \Phi_n(z) & \text{for } z \in (\varepsilon_n^-, \varepsilon_n^+) , \\ \\ +\infty & \text{for } z \notin (\varepsilon_n^-, \varepsilon_n^+) , \end{cases} \tag{23}$$

[4] As a matter of fact, a limitation of $\Gamma-$ convergence is that it can only capture global minima, thus disregarding the possibility of investigating bifurcations, local minima, as well as relevant saddle points. Willing to consider these aspects, the passage from molecular to continuum becomes more difficult.

and

$$G_n(w) \equiv \begin{cases} +\infty & \text{for } w \in (\varepsilon_n^- L/n, \varepsilon_n^+ L/n)\backslash\{0\} \ , \\ 0 & \text{for } w = 0 \, , \\ (L/n)\, \Phi_n \left(w/(L/n)\right) & \text{for } w \notin (\varepsilon_n^- L/n, \varepsilon_n^+ L/n) \ , \end{cases} \tag{24}$$

there exist functions F, $G : \mathbb{R} \to \mathbb{R} \cup \{+\infty\}$ such that

$$\Gamma - \lim_{n\to\infty} F_n^{**}(z) \equiv F(z) \ , \ \lim_{n\to\infty} G_n(w) \equiv G(w) \ , \tag{25}$$

where $F_n^{**}(\cdot)$ denotes the lower semicontinuous convex envelope[5] of $F_n(\cdot)$, and the notion Γ-lim is analogous to (17). Then, we have the following convergence result.

Theorem 1 . *Let* $\mathcal{E}[u]$ *be*

$$\mathcal{E}[u] = \begin{cases} \int_0^L \left[F(u'(x)) - f\,(x)\, u(x)\right] dx + \sum_{x_j \in J_u} G([u](x_j)) \, , \ u \in SBV(0,L) \ , \\ +\infty \qquad\qquad\qquad\qquad\qquad\qquad \textit{otherwise in } L^1(0,L) \ . \end{cases} \tag{26}$$

Then, $\mathcal{E}^n[u]$ *defined in (12)* Γ*-converges to* $\mathcal{E}[u]$ *for every* u*.*

The proof of this Theorem can be found in in [7]. Indeed, generalizations of this result (see [7]) are also possible, but in this introductory paper we have decided to state the simplest version, which applies best to our examples[6]. It should be mentioned that, in any case, the inelastic strain and fracture work do not disappear in the limit but are interpreted by function $G([u](x_j))$ in (26), which plays the role of the material cohesive fracture energy. Moreover, it is clear that regions of concavity for Φ_n, corresponding to softening branches in the interatomic force-displacement diagram, influence the shape

[5] The lower convex envelope f^{**} of a function f is defined as the largest lower-semicontinuos convex function which supports f from below.

[6] In general (21) and (22) may be also replaced by different growth conditions and in this case the limit energies are defined on broader function spaces. An alternative version of Theorem 1, relying on slightly different hypotheses, will be used in in Section 4.4.

of function $G(\cdot)$. It can be proved that $G(\cdot)$ is concave and, consequently, subadditive, i.e.

$$G(a) \leq G(\lambda\, a) + G((1-\lambda)\, a)\ ,\ \ \forall \lambda \in (0,1)\ , \tag{27}$$

whereas the bulk energy $F(\cdot)$ is always convex.

3.2 Analysis of the resulting continuum model.

Minimizers for functionals of the type (26) have been exhaustively discussed in [10], [11], [12] [13] and [9]; here we limit to recall the main conditions for their characterization. Consider a bar of length L with strain energy $\mathcal{E}[u]$ of the form (26). In the cases we consider, for reasonable choices of Ψ_1, we will always find $G(w) = +\infty$ for $w < 0$. Consequently, the minimization problem can be equivalently stated by considering the constraint

$$[u](x) > 0\ ,\ \forall x \in J_u\ , \tag{28}$$

which has the physical meaning of avoiding matter interpenetration. With boundary conditions $u(0) = 0$, $u(L) = \beta L$, we consider the problem of minimizing $\mathcal{E}[u]$, with u satisfying

$$\int_0^L u'(x)\, dx + \sum_{x \in J_u} [u](x) = \beta L\, . \tag{29}$$

Let u^* represent an equilibrium state for the bar. Considering for simplicity the only case in which $f = 0$ in (26), it has been proved in [12] that the non-negativeness of the first variation implies conditions

$$\begin{aligned} \frac{d}{dx}\left(F'(u^{*\prime}(x))\right) &= 0\ ,\ \ \forall x \in (0,L)\backslash J_{u^*}\ , \\ F'(u^{*\prime}(x)) &= G'([u^*](x))\ ,\quad \forall x \in J_{u^*}\ , \\ F'(u^{*\prime}(x)) &\leq G'(0^+)\, . \end{aligned} \tag{30}$$

In particular, $(30)_2$ has a very clear physical interpretation, i.e. $G'([u^*](\overline{x}))$ represents the cohesive axial force bridging the crack surfaces at $x = \overline{x}$.

The analysis of the second variation, characterizing local minimizers of the energy, provides the inequality [12]

$$F''(u^{*\prime}(x)) + L\,G''([u^*](x)) \geq 0\ , \quad \forall x \in J_{u^*}\ , \tag{31}$$

together with condition that there may be no more than one jump point with $G'' < 0$.

If we indicate with

$$\overline{\mathcal{E}}(\beta) = \min_{u(L)-u(0)=\beta L} \mathcal{E}[u]\ , \tag{32}$$

the energy stored in the bar when the relative displacement of its extremities is βL, the axial force $\overline{\sigma}$ is related to the average elongation β by

$$\overline{\sigma}(\beta) = \frac{1}{L}\frac{\partial}{\partial\beta}\overline{\mathcal{E}}(\beta)\,. \tag{33}$$

Determining $\overline{\mathcal{E}}(\beta)$ is particularly simple when the cohesive (fracture) energy G is strictly concave [12], i.e. both $F'(\cdot)$ and $G'(\cdot)$ are monotonic and, in addition, either $G(0^+) > 0$ or $G'(0^+) = +\infty$. In this case, there are only two possibilities: the bar equilibrium configurations may be either with no jumps or with one jump. In the first case, equations $(30)_{1-2}$ prescribe that

$$u^{*\prime}(x) = \beta\ ,\ \forall x \in (0,L)\ ;\ \ \overline{\mathcal{E}}(\beta) = LF(\beta)\ ,\ \ \overline{\sigma}(\beta) = F'(\beta)\ . \tag{34}$$

In the second case, if the jump of $u^*(\cdot)$ is at $x = \overline{x}$ and equal to $\overline{w}$, we find the characterization

$$\begin{aligned} u^{*\prime}(x) &= const = (F')^{-1}(G'(\overline{w}))\ ,\ \forall x \in (0,L)\backslash\overline{x}\,, \\ \beta &= (F')^{-1}(G'(\overline{w})) + \overline{w}/L\ . \end{aligned} \tag{35}$$

We will show with examples that the simultaneous presence of bulk and cohesive (fracture) energy may allow for stable softening branches in the average constitutive relation $\overline{\sigma}(\beta)$.

4 Examples.

We now apply our method to some representative examples.

4.1 Elasticity

The simplest case to be considered is that of an elastic response, described by a *convex* strain energy. Following the same rationale of Section 2, we consider chains formed by elementary springs of length λ with elastic energy per unit length

$$\Psi_1 = \frac{1}{\lambda} U\left(\frac{u_1 - u_0}{\lambda}\right) \ , \tag{36}$$

where $U(\cdot)$ is strictly convex and with a grow condition at infinity of order $p > 1$. It is a simple matter to show that considering chains of k springs whose ends are displaced apart of $(u_k - u_0) = \beta k \lambda$, the potential per-unit-length Ψ_k, defined as in (6), results to be

$$\Psi_k(\beta) \equiv \frac{1}{\lambda} U(\beta) \ , \ \forall k \, . \tag{37}$$

Therefore, the scaling law now leaves the potential invariant.

In order to apply Theorem 1, we may choose the thresholds ε_n^+ and ε_n^- appearing in (20), as $\varepsilon_n^{\pm} = \pm U^{-1}(n)$. Clearly the assumed growth of $U(\cdot)$ assures that hypotheses (20), (21) and (22) are satisfied. Moreover, recalling (23) (24), we easily find

$$F(z) = \frac{1}{\lambda} U(z) \ , \ G(w) = \begin{cases} 0 \, , & \text{if } w = 0 \, , \\ +\infty, & \text{otherwise} \, . \end{cases} \tag{38}$$

It follows that the resulting continuum model is an exact replica of the discrete model and fractures never appear. This result strongly depends on the fact that $U(\cdot)$ is strictly convex.

4.2 Griffith-type fractures

This case has been considered as the representative example in Section 2, and the discretization-dependent potentials Ψ_k are given by (7). Of course, instead of a parabola, any convex function with appropriate growth condition would give similar results. Referring to (8), we may choose the thresholds $\varepsilon_n^+ = (n)^{1/2} \varepsilon_{L/\lambda}$ and, $\varepsilon_n^- = -(n)^{1/2} \varepsilon_{L/\lambda}$ (indeed, the choice of ε_n^- is quite arbitrary). Applying the theorem, we obtain, recalling (4),

$$F(z) = a \, z^2 \, , \ G(w) \equiv \begin{cases} \lambda \, \gamma_1 & \text{if } w > 0 \, , \\ 0 & \text{if } w = 0 \, , \\ +\infty & \text{if } w < 0 \, . \end{cases} \tag{39}$$

It is interesting to notice that the resulting fracture energy for the continuous model is equal to that corresponding to the breaking of one single spring. Moreover, only opening fractures are contemplated.

The energy $\overline{\mathcal{E}}(\beta)$, introduced in (32) as a function of the average elongation β, results of the type

$$\overline{\mathcal{E}}(\beta) \equiv \begin{cases} a\,L\,\beta^2 & \text{if } \beta < \sqrt{\lambda\,\gamma_1/a}\,, \\ \\ \lambda\,\gamma_1 & \text{if } \beta \geq \sqrt{\lambda\,\gamma_1/a}\,. \end{cases} \tag{40}$$

and the corresponding average response $\overline{\sigma}(\beta)$ is readily found from (33).

4.3 Barenblatt-type brittle fractures

Suppose now that the elementary constituents are springs of length λ whose response is governed by a energy per-unit-length Ψ_1, formed by a convex and a concave branch. Despite the analysis could be developed in a very general way, here we consider an explicit example, where Ψ_1 reads

$$\Psi_1\,(\beta) = \begin{cases} \dfrac{\sigma_u}{2\varepsilon_1}\beta^2 & \text{for } \beta < \varepsilon_1\ , \\ \\ \dfrac{\sigma_u\varepsilon_1}{2} + \dfrac{\sigma_l(2\varepsilon_2 - \varepsilon_1 - \beta)(\beta - \varepsilon_1)}{2(\varepsilon_2 - \varepsilon_1)}\ , & \text{for } \ \varepsilon_1 \leq \beta < \varepsilon_2\ , \\ \\ \dfrac{\sigma_u\varepsilon_2}{2} + \dfrac{\sigma_l(\varepsilon_2 - \varepsilon_1)}{2}\ , & \text{for } \ \beta \geq \varepsilon_2\ , \end{cases} \tag{41}$$

with $\varepsilon_2 \gg \varepsilon_1$.

In Figure 6, the graph of $\Psi_1(\cdot)$ is juxtaposed to that of $\Psi_1'(\cdot)$, representative of the bar axial response. It should be noticed that there is a gap between the maximum axial load and the beginning of the softening branch in Figure 6_a, corresponding to a point of not-smoothness for $\Psi_1(\cdot)$.

For chains composed of $k+1$ atoms, that is for k springs, provided $\varepsilon_1 <$

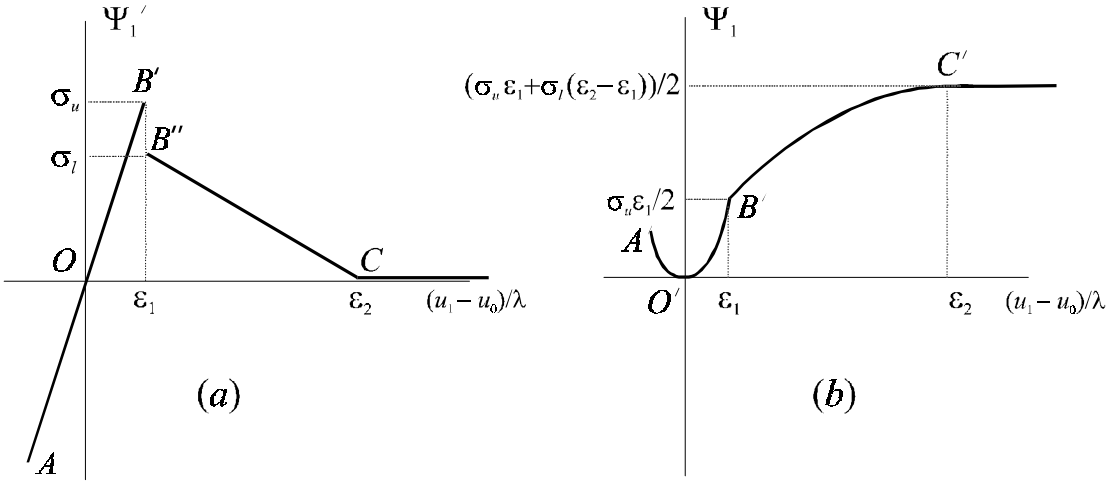

Figure 6: Axial response for a Barenblatt-type unit (a) and corresponding energy per unit length (b).

ε_2/k we obtain Ψ_k, defined as in (6), of the form

$$\Psi_k(\beta) = \begin{cases} \dfrac{\sigma_u}{2\varepsilon_1}\beta^2, & \text{for } \beta < \overline{\beta}\ , \\ Q_k(\beta)\ , & \text{for } \overline{\beta} \le \beta < \varepsilon_2/k\ , \\ \dfrac{1}{2\,k}\left(\sigma_u\varepsilon_1 + \sigma_l(\varepsilon_2-\varepsilon_1)\right)\ , & \text{for } \beta \ge \varepsilon_2/k\,, \end{cases} \tag{42}$$

where

$$Q_k(\beta) = \frac{k\sigma_l\sigma_u\,\beta(2\varepsilon_2 - k\beta) + \varepsilon_1(\varepsilon_2-\varepsilon_1)(\sigma_u-\sigma_l)^2 - k\varepsilon_1\sigma_l\left(\sigma_l(\varepsilon_2-\varepsilon_1)+\sigma_u\varepsilon_1\right)}{2k\left(\sigma_u(\varepsilon_2-\varepsilon_1)+\sigma_l\varepsilon_1 - k\sigma_l\varepsilon_1\right)}, \tag{43}$$

and

$$\begin{aligned} \overline{\beta} \;=\; & \frac{\varepsilon_1\varepsilon_2}{\varepsilon_2-\varepsilon_1\left(1-\dfrac{\sigma_l}{\sigma_u}\right)} \\ & \cdot\left[\frac{\sigma_l}{\sigma_u} + \left(1-\frac{\sigma_l}{\sigma_u}\right)\left(1-\frac{\varepsilon_1}{\varepsilon_2}\right)\sqrt{\frac{1}{k}\left(1+\frac{\sigma_l\varepsilon_1}{\sigma_u(\varepsilon_2-\varepsilon_1)}\right) - \frac{\sigma_l\varepsilon_1}{\sigma_u(\varepsilon_2-\varepsilon_1)}}\right]. \end{aligned} \tag{44}$$

Expression (42) provides the scaling law to pass from the discrete to a continuum model. As in Section 3, we consider a bar of length L, composed of $L/\lambda \gg 1$ atoms. Ideally subdividing the bar in n parts, we consider the sequence of approximating energies of the type (12), with now $\Phi_n(\cdot)$ obtained by posing $k = \frac{1}{n} L/\lambda$ in (42). We thus find

$$\Phi_n(\beta) = \begin{cases} \dfrac{\sigma_u}{2\varepsilon_1}\beta^2, & \text{for } \beta < e_1^{(n)} \ , \\ Q_{L/n\lambda}(\beta) \ , & \text{for } e_1^{(n)} \le \beta < n\, e_2 \ , \\ n\,\gamma_1 \ , & \text{for } \beta \ge n\, e_2 \, , \end{cases} \tag{45}$$

where $Q_{L/n\lambda}(\beta)$ is defined as in (43) with $k = \frac{1}{n} L/\lambda$,

$$\gamma_1 = \frac{\lambda}{2L}\left(\sigma_u \varepsilon_1 + \sigma_l(\varepsilon_2 - \varepsilon_1)\right) \ , \tag{46}$$

$$e_2 = \frac{\lambda}{L}\varepsilon_2 \, , \tag{47}$$

and

$$\begin{aligned} e_1^{(n)} &= \frac{\varepsilon_1 \varepsilon_2}{\varepsilon_2 - \varepsilon_1\left(1 - \dfrac{\sigma_l}{\sigma_u}\right)} \\ &\quad \cdot \left[\frac{\sigma_l}{\sigma_u} + \left(1 - \frac{\sigma_l}{\sigma_u}\right)\left(1 - \frac{\varepsilon_1}{\varepsilon_2}\right)\sqrt{\frac{n\lambda}{L}\left(1 + \frac{\sigma_l \varepsilon_1}{\sigma_u(\varepsilon_2 - \varepsilon_1)}\right)} - \frac{\sigma_l \varepsilon_1}{\sigma_u(\varepsilon_2 - \varepsilon_1)}\right] \\ &= C_1\left(1 + C_2\sqrt{n - C_3}\right), \end{aligned}$$

with C_1, C_2 and C_3 positive constants and $C_3 < 1$. The corresponding graphs are shown in Figure 7 for small values of n.

In order to apply Theorem 1 we choose

$$\varepsilon_n^{\pm} = \pm e_1^{(n)}. \tag{48}$$

It is easy to verify that conditions (20), (21) and (22) are simultaneously satisfied for some a, C and $p = 2$. From definitions (23) and (24) we find

$$F(z) = \frac{\sigma_u}{2\varepsilon_1} z^2 \tag{49}$$

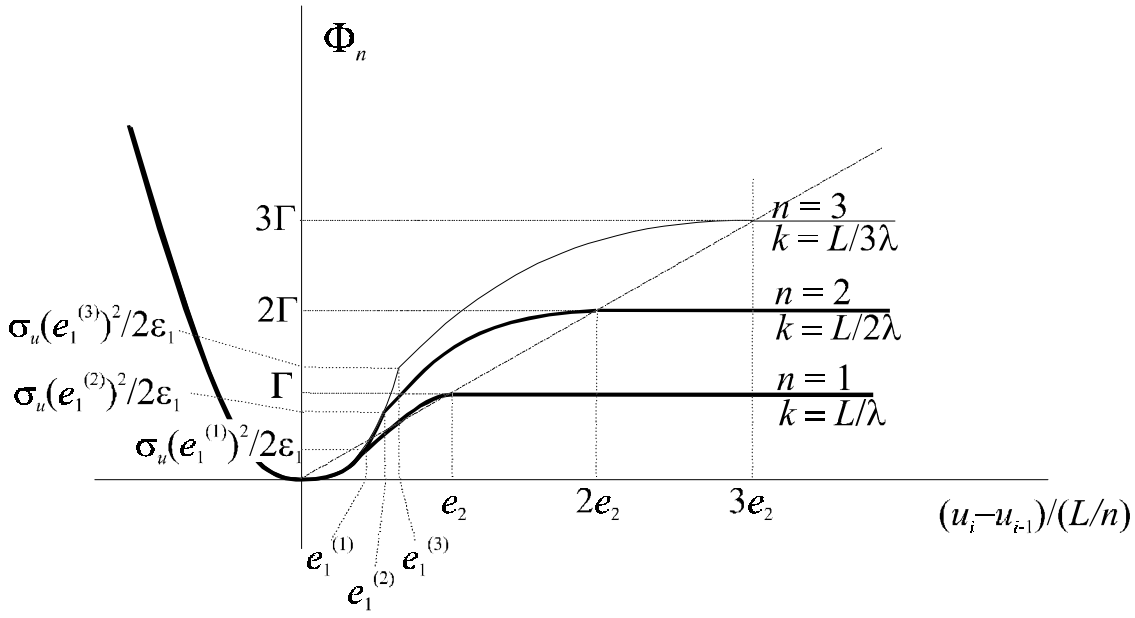

Figure 7: Scaling law for Barenblatt–type elements.

and

$$G(w) = \begin{cases} +\infty\,, & \text{for } w < 0\,, \\ 0\,, & \text{for } w = 0\,, \\ \dfrac{\sigma_l\sigma_u\,(2\varepsilon_2 - w/\lambda)\;w + \lambda\,\varepsilon_1(\varepsilon_2 - \varepsilon_1)(\sigma_u - \sigma_l)^2}{2\,(\sigma_u(\varepsilon_2 - \varepsilon_1) + \sigma_l\varepsilon_1)}\,, & \text{for } 0 < w < \lambda\,\varepsilon_2\,, \\ \dfrac{\lambda}{2}\,(\sigma_l(\varepsilon_2 - \varepsilon_1) + \sigma_u\varepsilon_1) \equiv \gamma_1\,, & \text{for } w \geq \lambda\,\varepsilon_2\,. \end{cases} \tag{50}$$

The graphs of $F(\cdot)$ and $G(\cdot)$ are reported in Figure 8.

The limit continuous energy $\mathcal{E}[u]$, having the same properties stated in Section 3, is given by

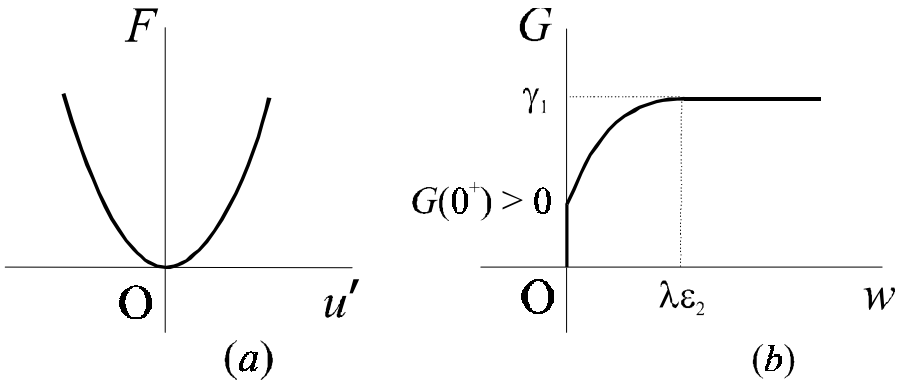

Figure 8: Graphs of the bulk (a) and fracture (b) energies for the continuum model.

$$\mathcal{E}[u] = \begin{cases} \int_0^L [F(u'(x))]\, dx + \sum_{x_j \in J_u} G([u](x_j))\,, \ u \in SBV(0,L)\,, \\ \\ +\infty \qquad\qquad\qquad\qquad\qquad \text{otherwise in } L^1(0,L)\,. \end{cases} \tag{51}$$

The corresponding average stress-strain curves have been discussed in [12]. As already mentioned in Section 3.2, there are only two possibilities: uncracked bar ($N = 0$) or only one crack ($N = 1$). The energy corresponding to $N = 0$ can be calculated from (34) and is represented by the convex branch in Figure 9_a. The corresponding graph of $\overline{\sigma}(\beta)$, becoming a straight line in the particular case of quadratic bulk energies $F(\cdot)$, is reported in Figure 9_b.

For $N = 1$, the quantities $\overline{\mathcal{E}}(\beta)$ and $\overline{\sigma}(\beta)$ can be calculated from (35). Now the gross response is influenced by the bar length L (size effect) and we have to distinguish two situations. When the bar is short, in particular when

$$L < L_0 \equiv \lambda \frac{\sigma_u(\varepsilon_2 - \varepsilon_1) + \sigma_l \varepsilon_1}{\sigma_l \varepsilon_1}, \tag{52}$$

denoting with β_e the bulk strain corresponding to the incipient crack opening, i.e. $F'(\beta_e) = G'(0^+)$, we have from (52) that $\beta_e < \lambda\varepsilon_2/L$ and the graphs of $\overline{\mathcal{E}}(\beta)$ and $\overline{\sigma}(\beta)$ are of the type represented in Figure 9. In particular, $\overline{\mathcal{E}}(\beta)\big|_{N=0} = \overline{\mathcal{E}}(\beta)\big|_{N=1}$ at $\beta = \beta_m$, with $\beta_m > \beta_e$. Consequently, it is then

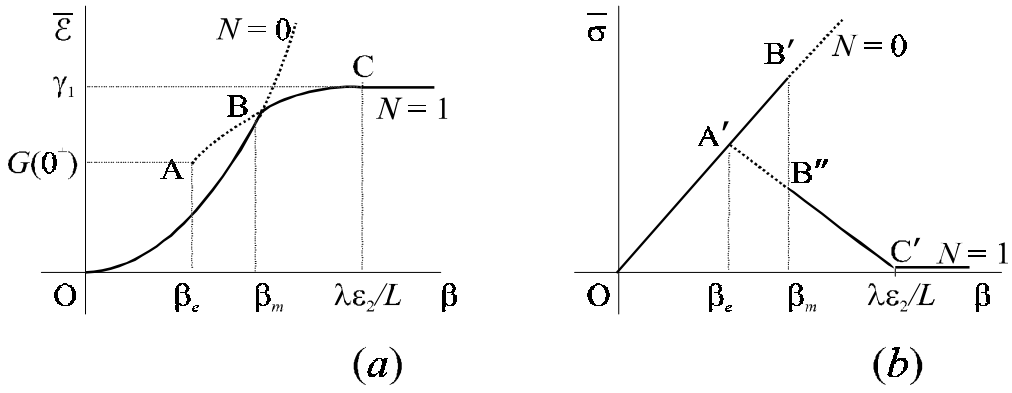

Figure 9: Energy $\overline{\mathcal{E}}(\beta)$ and axial force $\overline{\sigma}(\beta)$ as a function of average elongation β for short bars ($L < L_0$).

clear that the uncracked configuration is metastable for $\beta > \beta_m$. The bar response will follow the linear branch OB′ in Figure 9_b up to B′, where it jumps to B″ belonging to the cracked ($N = 1$) branch; increasing β, the bar exhibits strain softening from B″ to C′ and, eventually, results completely broken after C′ ($\beta > \lambda\varepsilon_2/L$). The distance B′B″ results to be an increasing function of the bar length L.

A different situation occurs when (52) is not satisfied, which means that $\beta_e > \lambda\,\varepsilon_2/L$. The stress decrease which accompanies the development of a crack implies a release of the whole bar but now, since the bar is long, the average elongation β reduces as the crack opens. Consequently, the $\overline{\mathcal{E}}(\beta)\big|_{N=1}$ path proceeds leftward, from point A to point C in Figure 10_a. The bar shows the tendency to snap-back. The stable-equilibrium response follows the path OB′B″D′ in 10_b.

4.4 Barenblatt-type ductile fractures

A particular response can be obtained for a borderline case of the constitutive relation (41). Now the elementary springs have an energy per unit length Ψ_1

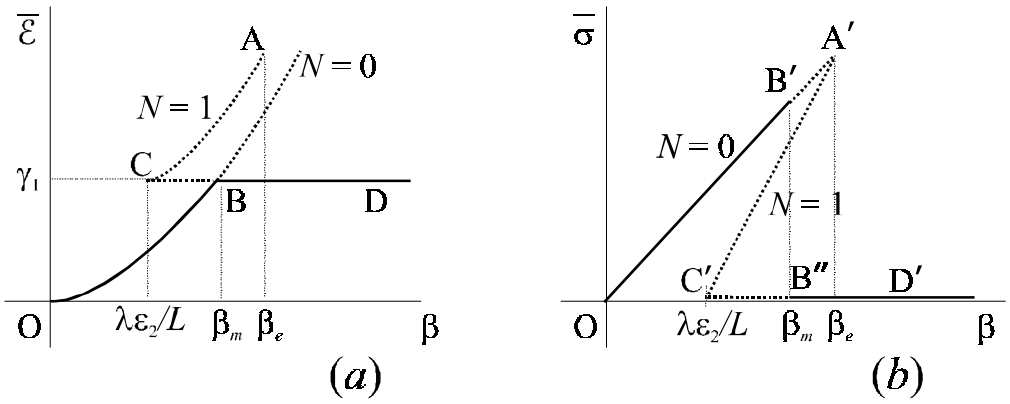

Figure 10: Energy $\overline{\mathcal{E}}(\beta)$ and axial force $\overline{\sigma}(\beta)$ as a function of average elongation β for long bars ($L > L_0$).

defined by

$$\Psi_1(\beta) = \begin{cases} \dfrac{\sigma_1}{2\varepsilon_1}\beta^2 & \text{for } \beta < \varepsilon_1 \ , \\ \dfrac{\sigma_1\varepsilon_2}{2} - \dfrac{\sigma_1}{2(\varepsilon_2-\varepsilon_1)}(\varepsilon_2-\beta)^2 & \text{for } \varepsilon_1 \le \beta < \varepsilon_2 \ , \\ \dfrac{\sigma_1\varepsilon_2}{2} & \text{for } \beta \ge \varepsilon_2 \ , \end{cases} \tag{53}$$

with $\varepsilon_2 \gg \varepsilon_1$. The only difference with the previous case is that we have posed $\sigma_u = \sigma_l = \sigma_1$ in (41). The graphs of $\Psi_1(\cdot)$ and $\Psi_1'(\cdot)$ are shown in Figure 11.

For chains composed of $k+1$ atoms (k springs), provided $\varepsilon_1 < \varepsilon_2/k$, we get for Ψ_k, defined in (6),

$$\Psi_k(\beta) = \begin{cases} \dfrac{\sigma_1}{2\varepsilon_1}\beta^2, & \text{for } \beta < \varepsilon_1 \ , \\ \dfrac{\sigma_1}{2}\left[\varepsilon_2/k - \dfrac{(\beta-\varepsilon_2/k)^2}{\varepsilon_2/k-\varepsilon_1}\right] & \text{for } \varepsilon_1 \le \beta < \varepsilon_2/k \ , \\ \dfrac{\sigma_1\varepsilon_2}{2k} \ , & \text{for } \beta > \varepsilon_2/k \, . \end{cases} \tag{54}$$

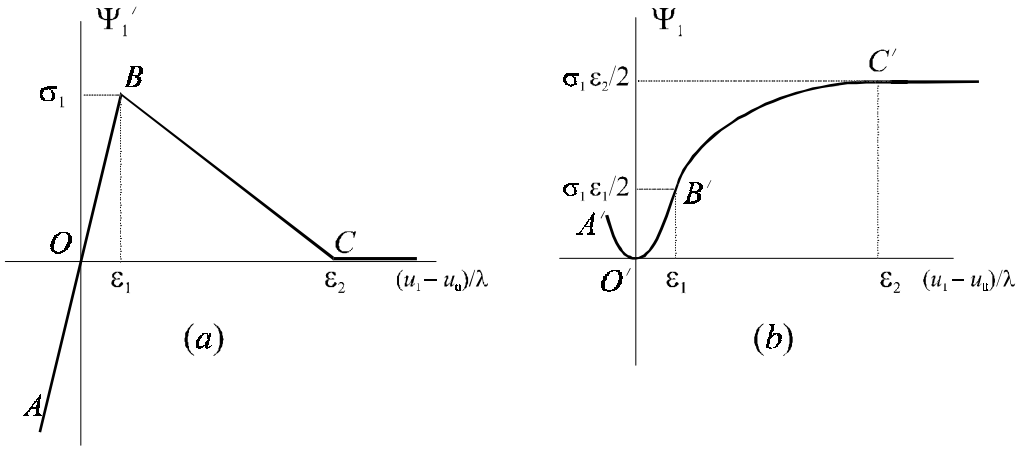

Figure 11: Axial response for a particular Barenblatt-type unit (a) and corresponding energy per unit length (b).

Thinking of the bar of length L as composed of n parts, we consider the sequence of approximating energies $\Phi_n(\cdot)$, obtained by posing $k = \frac{1}{n}L/\lambda$ in (42), whose graphs are shown in Figure 12 for $n = 1, 2, 3$.

On the contrary to what happened in Figure 7, now the basin of convexity is delimited by the value ε_1. Consequently, it is not possible to find thresholds $\varepsilon_n^{\pm}$ so that conditions (20), (21) and (22) are simultaneously satisfied. However, we can apply a slightly modified version of Theorem 1 to get a continuous energy $\mathcal{E}[u]$ with the same properties stated in Section 3 (the technical result we are going to use can be found in detail in [7]). For, let us choose $\varepsilon_n^{\pm} = \pm\sqrt{n}\varepsilon_2/(L/\lambda)$ and consider F_n and G_n defined in (23) and (24). It can be proved that the limits F and G defined in (25) are now given by

$$F(z) = \begin{cases} \dfrac{\sigma_1}{2\varepsilon_1} z^2 \ , & \text{for } z \le \varepsilon_1 \ , \\ \\ \sigma_1(z - \varepsilon_1) + \dfrac{\sigma_1 \varepsilon_1}{2\varepsilon_1} \ , & \text{for } \ z > \varepsilon_1 \, , \end{cases} \tag{55}$$

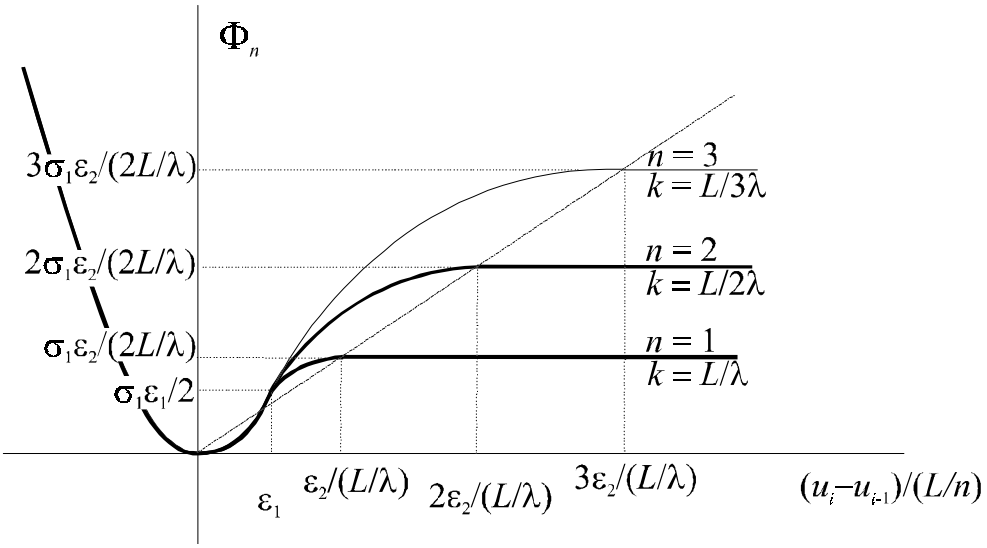

Figure 12: Scaling law for chains composed of the Bareblatt-type elements of Figure 11.

$$G(w) = \begin{cases} +\infty\ , & \text{for } w < 0\ . \\ \dfrac{\sigma_1\varepsilon_2}{2}\lambda\left(1-\left(1-\dfrac{1}{\varepsilon_2}\dfrac{w}{\lambda}\right)^2\right), & \text{for } 0 \le w \le \lambda\,\varepsilon_2\ , \\ \dfrac{\sigma_1\varepsilon_2}{2}\lambda\ , & \text{for } w > \lambda\varepsilon_2\ . \end{cases} \tag{56}$$

The graphs of F and G are similar to that in Figure 8, except that now $G(0^+) = 0$. Using the results of [7], the energy for a continuous bar reads

$$\mathcal{E}[u] = \begin{cases} \displaystyle\int_0^L [F(u'(x)) - f\,(x)\,u(x)]\ dx \\ \quad + \displaystyle\sum_{x_j \in J_u} G([u](x_j)) \ + \sigma_1 |D^c u|(0,L)\ , & \text{for } u \in BV(0,L)\ , D^c u \ge 0\ , \\ +\infty & \text{otherwise in } L^1(0,L)\ . \end{cases} \tag{57}$$

It should be mentioned that condition $G(0^+) = 0$ enlarges the space of admissible function from $SBV(0, L)$ to $BV(0, L)$. We briefly recall that $BV(0, L)$ consists of functions that can be written in the form $u = v + \varphi$, where v belongs to the space $SBV(0, L)$ already introduced, and φ is a Cantor-type function (see [17], Chap. 9, Sect. 33.1), i.e., a continuous function whose (distributional) derivative is a non-atomic measure, singular with respect to the 1-dimensional Lebesgue measure. We denote with $D^c u$ the distributional derivative of φ. Typically, the support of $D^c u$ has a *fractal* dimension. The quantity $|D^c u|(0, L)$ denotes the total variation [17] of the measure $D^c u$ on the set $(0, L)$ and can be interpreted as a *diffused damage* in the bar.

The rigorous mathematical analysis of minimizers of (57) goes beyond the purpose of this paper and can be found with detail in [9]. However, we have mentioned this example here since, for the particular energy defined by (55) and (56), for any β we can find at least a minimizer of (57) that belongs to $SBV(0, L)$. Its characterization makes use of (34) and (35) and is analogous to the previous case. For, we have again to distinguish the case of long and short bars. The graphs of $\overline{\mathcal{E}}(\beta)$ and $\overline{\sigma}(\beta)$ are represented in Figure 13. For long bars the response is similar to that of Section 4.3, exhibiting snap-back. The stable equilibrium path is $\mathrm{OB}'_{(l)}\mathrm{B}''_{(l)}\mathrm{D}'_{(l)}$, represented in Figure 13$_b$.

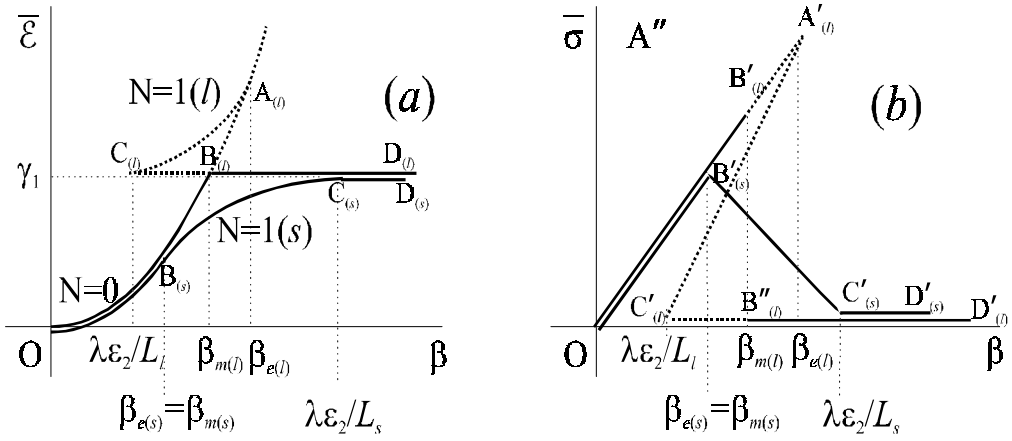

Figure 13: Energy $\overline{\mathcal{E}}(\beta)$ and axial force $\overline{\sigma}(\beta)$ as a function of average elongation β.

On the other hand, the response of short bars is represented, in the same

Figure, by $OB'_{(s)}C'_{(s)}D'_{(s)}$. What should be noticed is that there is a smooth transition from point $B'_{(s)}$ to $C'_{(s)}$, i.e. now the opening of a crack depends continuously on β[7]. In other words, in an experiment on short specimens, the opening of the crack could be directly "controlled" by the testing machine stroke. This response is characteristic of ductile fracture.

5 Conclusions

Despite its simplicity, the 1-D chain of nearest-neighbor interacting atoms is a model evidencing that, in general, the passage from a molecular (discrete) to a continuum theory is a ticklish step. The difficulties are particularly evident when the atomic potential presents points of non-convexity, corresponding to softening branches in the corresponding force-displacement relationship.

Here we have presented a mathematical approach to the problem that, in engineering terms, may be so summarized. In the one-dimensional case, we consider chains composed of a great number of interacting atoms and we attempt a limit theory for a homogenized continuous bar, where each representative volume element is supposed to be a sub-chain containing a sufficiently high number of atoms. The limit is obtained through three steps: *i*) evaluation of the size-effect scaling law for the uniaxial response of chains made of a great number of atoms, as the chain length (and consequently the atom number) is diminished; *ii*) extrapolation of the scaling law beyond the threshold of physical significance, i.e. when the chain becomes smaller than the atomic spacing; *iii*) use of a mathematical procedure (Γ-convergence of difference schemes) to conceive a continuum model by letting the length of the representative volume element go to zero. The most important consequence in *i*) is that the basin of stability of the chain overall potential-energy, as well as its minimum value in the concave (unstable) region, progressively grow as the length of the chain is diminished.. In step *ii*) we extrapolate the scaling law determined in *i*) keeping track of its trend as the length of the representative volume element goes to zero. As a result, we obtain an unbounded growth that has no physical justification, since the length of the representative volume element cannot be smaller than the atomic spacing, but acquires the same value of a mathematical limit, in the sense that we consider the function "trend" in a neighborhood of the limit point, rather

[7] The fact that the snap-back response, for smooth non-convex potentials, is indeed a structure (size) effect, had been noticed in [23] for discrete one-dimensional atomic chains.

than the value of the function *at* the limit point. Using the mathematical tool *iii*), we thus obtain a continuous bar that has the same characteristic properties of the discrete model (in particular with the same fracture energy) and, what is more, is mesh-independent. The key-point for this is consideration of a mesh dependent constitutive law, which is interpreted as the natural size-effect re-scaling..

The atomic chain model may also stimulate, by insight, some conjectures about the mechanical characterization of real materials. In particular, it is well known that any response obtainable through uniaxial tests is size-dependent. In fact, since the macroscopic response is due, in general, to underlying microstructural rearrangements (grain slipping, dislocation movements, fiber debonding etc.) it is clear that the smallest representative volume element cannot be of vanishing size, being instead characterized by an intrinsic length scale. How to measure this intrinsic length scale? How to define an intrinsic constitutive law, valid for an equivalent continuum, starting from size-dependent experimental responses.

The definition of a strategy to give at least a partial answer to the aforementioned questions may draw inspiration from our 1-D example. Our analysis of discrete element chains suggests that an "intrinsic" equivalent-continuum constitutive relationship (between local stress and local strain) can be defined starting from average-stress vs. average-strain diagrams (obtained through simple uniaxial tests). But what is of crucial important is consideration of the scaling (size) effect as the specimen length is varied. Our model problem suggests that *it is such a scaling that implicitly defines properties correlated to the material underlying microstructure and its internal length scale.* The extrapolation and manipulation of the scaling laws, as illustrated in Section 3 (using Γ-convergence), provides a possible strategy (of course not the only one possible) to pass to the limit as the specimen length goes to zero, eventually conceiving a continuum model. The resulting continuum is *equivalent* to the discrete ensemble, in the sense that it presents the same characteristics (fracture energy, size effect) of the discrete arrangement.

A continuous body is nothing but a mathematical abstraction, since any real material, at a closer examinations, reveals instead the structure of grains, crystal, complex molecules, interacting the one with the other. But notice that even in the case of an ideal continuous bar, it would be impossible to measure its constitutive law, suppose unknown, through uniaxial tests. In fact, in any feasible test, we may only impose certain displacements to a

discrete set of points[8] and measure the work consumed in the consequent deformation. In other words, only approximations of the strain energy, of the type (12), can be directly measured. But we may use our method to pass to the limit as $n \to \infty$ in functionals (12) to obtain the constitutive law of the continuum. We may imagine to calculate such limit through a program of more and more refined tests, i.e. by increasing the number of gauge points where the displacement is imposed.

We have also found that the energy functional we obtain in the continuum limit consists as a rule, as shown in (26), of two parts: a bulk strain energy F, operating on the displacement gradient, and a cohesive fracture energy G, which is a function of the jump amount wherever the displacement is discontinuous. The discontinuity interprets the occurrence of cracking in the body. We have also observed that the average response of bars obeying to such strain energy may apparently show stable softening branches. We say "apparently" because softening is the macroscopic consequence of crack opening, i.e. the crack opening smeared along the whole bar length. Consequently, it would be completely erroneous to assume the average response as an approximation of the local response.

It should be mentioned that the importance of a distinction between bulk and fracture response has been already noticed by many authors. In particular, as exhaustively discussed by Del Piero [11], it is the shape of the fracture energy G that greatly influences the material gross response: for example, just slightly changing G while maintaining F fixed, a smooth transition from ductile to brittle behavior for tensile bars may be obtained.

Finally, it is worth recalling that in the crack band model proposed by Bažant as a localization limiter [5], fracture is assumed to be confined in a band of finite length. In Bažant's model, the cohesive forces connecting the crack surfaces must re-scale as the width of the crack band is varied [5], suggesting again the importance of the separation of scale in all the theories. From the point of view of our theory, the fracture energy term G represents, in rough terms, a borderline case of Bažant's crack-band model when the band width tends to zero.

Acknowledgements. Motivation for this work started from a very stimulating discussion with Professor I. Iori (University of Parma). This research was conducted while G. R. C. was visiting the Scuola Normale

[8] Using for example a testing device of the type represented in Figure 5.

Superiore in Pisa as a guest of Professor L. Ambrosio, who is gratefully thanked for his precise suggestions and for having encouraged the collaboration of the authors. We would also like to acknowledge Professors Z. Bažant (Northwestern University), K. Bhattacharya (California Institute of Technology), A. Braides (University of Rome II) and L. Truskinovsky (University of Minnesota), for their valuable advice during the preparation of this work.

References

[1] Bažant, Z., Instability, ductility and size-effect in strain-softening concrete, *J. Eng. Mechanics ASCE*, **102**, pp.331-344, 1976 (Discussion, **103**, pp.357-358, pp. 775-777 and **103**, pp.501-502).

[2] Bažant, Z. and Belytschko, T., Wave propagation in strain softening bars: exact solutions, *J. Eng. Mechanics ASCE*, **111**, 381-389, 1985.

[3] Bažant, Z. and L. Cedolin, *Stability of Structures: Elastic, Inelastic, Fracture and Damage Theories*, Oxford University Press, New York, 1991.

[4] Bažant, Z. and Chen, E. P., Scaling of structural failure, *Appl. Mech. Rev.*, **50**(10), pp. 593-627, 1997.

[5] Bažant, Z. and Planas, J., *Fracture and Size Effect in Concrete and Other Quasi-Brittle Materials*, CRC press, New York, 1998.

[6] Braides, A., Γ-*convergence for Beginners*, Oxford University Press, in press, 2001.

[7] Braides, A., and Gelli, M.S., Continuum limits of discrete systems without convexity hypotheses, *Mathematics and Mechanics of Solids*, in press, 2001.

[8] Braides, A., and Gelli, M.S., *From Discrete to Continuum: a Variational Approach.* Lecture Notes, SISSA, Trieste, 2000 (available on the server `http://www.sissa.it/fa/pubblications/pub.html`).

[9] Braides, A., Dal Maso, G., Garroni, A., Variational formulation of softening phenomena in fracture mechanics: the one-dimensional case, *Arch. Rat. Mech. and Analysis*, **146**, pp.23-58, 1999.

[10] Choksi, R., Del Piero, G., Fonseca, I., Owen, D., Structured deformations as energy minimizers in models of fracture and hysteresis, *Mathematics and Mechanics of Solids*, **4**(3), pp.321-356, 1999.

[11] Del Piero, G., One-dimensional ductile-brittle transition, yielding and structured deformations. In Argoul, P., Frèmond, M., Nguyen, Q.S. (EDS), *Variations de domaines et frontières libres en mécanique des solides*, Kluwer, Dordrecht, 1999.

[12] Del Piero, G., Truskinovsky, L., A one-dimensional model for localized and distributed fractures, *J. de Physique IV*, **8**, pp. 95-102, 1998.

[13] Del Piero, G., Truskinovsky, L., Macro- and micro-cracking in one dimensional elasticity, *Int. J. Solids and Structures*, **38**, pp. 1135-1148, 2001.

[14] Dunn, J. E. and R. Fosdick, The morphology and stability of material phases, *Arch. Rat. Mech. Anal.*, **74**, pp.1-99, 1980.

[15] Ericksen, J. L., Equilibrium of bars, *J. of Elasticity*, **5**, pp. 191-202, 1975.

[16] Ericksen, J. L., Ill-posed problems in thermoelasticity theory, in *System of Non-linear Partial Differential Equations*, J.M. Ball Editor, pp. 71-93, Dordrecth, 1983.

[17] Kolmogorov, A. N., Fomin, S. V., *Introductory Real Analysis, Dover, New York*, 1975.

[18] Kondepudi, D. and I. Prigogine, *Modern Thermodynamics*, John Wiley and Sons, Chichester, 1998.

[19] Meyer, C. and Okamura, H., eds., *Finite Element Analysis of Reinforced Concrete Structures*, ASCE, New York, 1986.

[20] Müller, I. and P. Villaggio, a Model for an elastic plastic body, Arch. Rat. Mech. Analysis, **25**, pp. 25-46, 1977.

[21] Rogers, R.C. and L. Truskinovsky, Discretization & hysteresis, *Physica B*, **233**, pp.370-375, 1997.

[22] Royer-Carfagni, G., Can a Moment-Curvature Relation Describe Flexural Behavior of Softening Beams?, *European Journal of Mechanics A-Solids*, **20**, pp. 253-276, 2001.

[23] Truskinovsky, L., Fracture as a phase transition, in *Contemporary Research in the Mechanics and Mathematics of Materials*, Batra, R. C., and Beatty, M. F., Eds., pp. 322-332, CIMNE, Barcelona, 1996.

[24] Young, L.C., *Lectures on the calculus of variations and optimal control theory*, Saunders, Philadelphia,1969.